Pin-fin shape and orientation effects on wall heat transfer predictions of gas turbine blade

Cite as: AIP Conference Proceedings **2114**, 020008 (2019); https://doi.org/10.1063/1.5112392
Published Online: 26 June 2019

Marwan Effendy, Yufeng Yao, Jun Yao, and Denis R. Marchant

Pin-fin Shape and Orientation Effects on Wall Heat Transfer Predictions of Gas Turbine Blade

Marwan Effendy[1, a)], Yufeng Yao [2)], Jun Yao [3)] and Denis R Marchant [4)]

[1]Department of Mechanical Engineering, Universitas Muhammadiyah Surakarta, Pabelan, Kartasura, Surakarta, Indonesia.
[2]Department of Engineering Design and Mathematics, University of the West of England, Coldharbour Lane, Bristol BS16 1QY, United Kingdom.
[3]School of Engineering, University of Lincoln, Brayford Pool, Lincoln LN6 7TS, UK
[4]Faculty of Science, Engineering and Computing, Kingston University London, Penrhyn Road, Kingston upon Thames KT1 2EE, United Kingdom.

a) Corresponding author: Marwan.Effendy@ums.ac.id

Abstract. Turbine blades are often exposed to the 'hot' gas environment and thus it is essential to apply effective cooling technique to extend the blade lifetime. In the present work, wall heat transfer characteristics inside a blade trailing-edge coolant passage were investigated by analyzing two baseline configurations experimentally studied by previous researchers. In addition, three new configurations were proposed by varying shape and orientation against an incoming airflow. All these five configurations adopted similar layout with five-row elliptic pin-fins in the main coolant region and one-row fillet circular pin-fin in the exit region. Validation study was started by two baseline configurations by comparing CFD predictions with experimental measurements, followed by wall heat transfer predictions of three newly proposed configurations. It was found that pin-fin shape and its orientation have considerable effects on the wall heat transfer characteristics, and that by rotating the pin-fin against incoming flow, some compromises could be achieved, such as higher heat transfer coefficient and lower pressure loss.

INTRODUCTION

The performance of a gas turbine engine, e.g. the power output and thermal efficiency, could be increased significantly with the increase of mixture gases temperature at the inlet. This results in a turbine operating at temperatures in excess of the melting point of the material that made a blade. To avoid blade deformation or damage and to extend its lifetime, blade cooling techniques need to be used, such as internal and film cooling systems via convection, conduction and transpiration among other approaches. A common practice to enhance heat transfer performance of a blade internal coolant passage is to insert small obstacles, i.e., pin-fins, ribs or other objectives in order to increase surface areas as well as to promote the near-wall turbulence intensity level. In the past, blade coolant passage performance has been studied experimentally and numerically for various configurations of staggered and/or in-line arrangements with cylindrical pin-fins [1][3], elliptical pin-fins [4][5], streamwise elliptical pin-fins [6][7], spanwise elliptical pin-fin [8][9], double in-line ribs array [10][11]. Han and Rallabandi [12] reviewed the latest developments on the turbine blade cooling techniques. A patent proposed by Martin *et al*. [13] also demonstrated a turbine blade design with novel multiple trailing-edge cooling holes, aiming for an effective cooling system solution that can keep the blade metal temperature below the critical value during normal and over-loading operation conditions.

There are wide ranges of pin-fin geometries, such as elliptic, circular, square, aerofoil, drop form, and lancet, which can be used for internal coolant passage. Moreover, some have been investigated numerically and experimentally in term of total pressure drop (friction loss) and wall heat transfer coefficient. It was found that to achieve the efficiency and effectiveness of a blade internal cooling system, it is important to improve the coolant

Exploring Resources, Process and Design for Sustainable Urban Development
AIP Conf. Proc. 2114, 020008-1–020008-8; https://doi.org/10.1063/1.5112392
Published by AIP Publishing. 978-0-7354-1850-9/$30.00

passage heat transfer performance. This can be attained by raising turbulence levels, increasing coolant flow unsteadiness, while minimizing the total pressure loss [14]. Innovated trailing-edge internal cooling designs with a pentagonal arranged circular pin-fin and staggered elliptical pin-fin [8]. Turning flow effect in front of cooling passage on blade cooling system with enlarged pedestals and square or semicircular ribs was numerically investigated by Facchini *et al*. [15].

The present study is to investigate the effect of pin-fin shape and orientation on cooling performance, based on variants of two earlier experimental configurations. CFD study will be carried out to quantify the performance of a total of five configurations as summarized in Table 1 below, including two baseline configurations (G5N21, G5N22) of Tarchi's experiments and three newly proposed configurations (G5N10, G5N23, G5N24) for performance comparisons.

TABLE 1. Summary of present case studies

Design	Pin-fin shape	Orientation	S/D	S_x/D	D=H (mm)	Re_{L0}
G5N10	circular	Staggered	2.5	2.17	6.72	9,000 – 35,900
G5N21	elliptic	streamwise staggered	2.5	2.17	6.72	9,000 – 27,000
G5N22	elliptic	spanwise staggered	2.5	2.17	6.72	13,000 – 35,900
G5N23	elliptic	in-line staggered (45^o)	2.5	2.17	6.72	9,000 – 35,900
G5N24	elliptic	counter-rotating staggered (45^o)	2.5	2.17	6.72	9,000 – 35,900

DOMAIN, MESHING AND BOUNDARY CONDITIONS

Geometries

Two configurations experimentally studied by Tarchi *et al*. [8] were considered; i.e. streamwise staggered elliptical pin-fin (G5N21) and spanwise staggered elliptical pin-fin (G5N22), respectively. Based on the G5N21 and the G5N22 configurations, three new configurations were proposed by replacing elliptical pin-fin with circular shape (G5N10), and changing the angle of elliptic pin-fin against incoming flow to 45^o degrees with in-line arrangement (G5N23) or counter-rotating arrangement (G5N24), as seen in Fig. 1. All five configurations consist of five-row pin-fin in the L_1 region and one-row fillet circular pin-fin in the L_2 region, each row having 12 or 11 pin-fins in the lateral direction of a total width of 200mm and being fitted into a 10^o wedge-shape duct. The pin-fin has a diameter or minor axis length of H=6.72 mm and a fillet radius of r=0.5H.

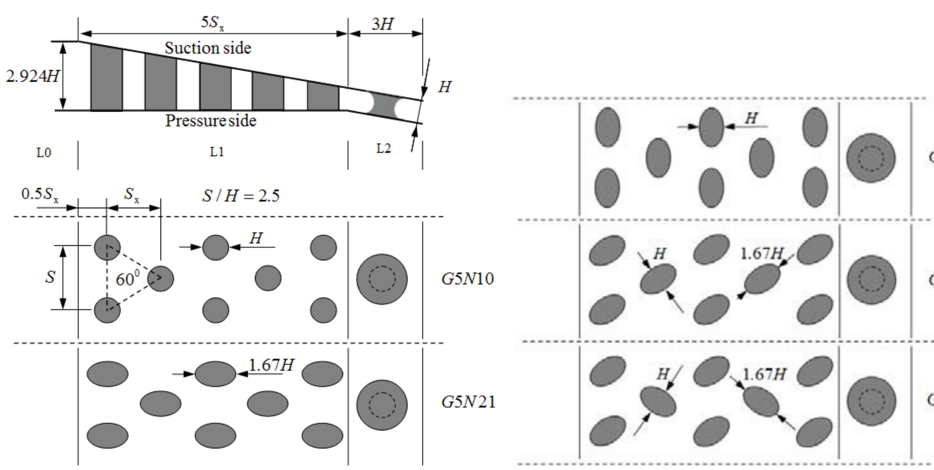

FIGURE 1. Geometries and configurations

Meshing

The computational grids were constructed by using CFX-meshing tool in ANSYS® 12.1 workbench. Unstructured meshes were applied for all configurations, resulting in 5.2-5.6 million elements. Actually, these meshes could be minimized by applying the structured mesh as used in the numerical study of wall heat transfer and pressure loss of streamwise staggered elliptical pin-fin [7]. The mesh characteristics of a full computational domain are summarized in Table 2.

TABLE 2. Mesh Characteristics

Description	G5N10	G5N21	G5N22	G5N23	G5N24
Mesh size (elements)	5,517,747	5,343,265	5,215,696	5,259,052	5,272,198
Nodes	2,236,991	2,211,456	2,152,098	2,165,624	2,160,811
Tetrahedrons	1,747,504	1,562,291	1,544,834	1,570,405	1,605,188
Wedges	3,725,679	3,717,308	3,607,102	3,621,538	3,595,776
Pyramids	44,564	63,666	63,760	67,109	71,234
Aspect ratio (max)	19.74	19.70	19.78	19.82	19.94
y^+ end wall (average)	2.15	2.18	3.44	2.66	2.63
y^+ pin fin (average)	1.97	1.92	3.54	2.28	2.69

Flow and boundary conditions

Numerical studies consider exactly the same conditions as the experiments; i.e. for each case tuning back pressure to target an averaged Mach number of 0.3 at the 5^{th} row throat section and the corresponding Reynolds number varied between 9,000 and 36,000. There are two types of simulations; namely the 'cold' test for passage pressure loss and the 'warm' test for wall heat transfer. For both simulations, surface roughness of 5 and 1.5microns were applied for the end-walls and pin-fin surfaces and this refers to the transparent material for end-walls and the aluminum for pin-fin walls. The inlet turbulence intensity was set to be a medium level of 5%.

DEFINITION AND ANALYTICAL FORMULA

Reynolds and Nusselt numbers

The Reynolds number (Re) and Nusselt number (Nu) are formulated in two different manners, the first is referred to pin-fin diameter (D) and the second is based on the hydraulic diameter of inflow section (L_0) as:

$$Re_{\mathrm{d}} = \frac{\dot{m}D}{A_{\min}\mu}, \qquad \text{and } Nu_{\mathrm{d}} = \frac{hD}{k} \tag{1}$$

$$Re_{\mathrm{L0}} = \frac{\dot{m}D_{\mathrm{L0}}}{A_{\mathrm{L0}}\mu}, \qquad \text{and } Nu_{\mathrm{L0}} = \frac{hD_{L0}}{k} \tag{2}$$

Where Re_d and Re_{L0} are the Reynolds number at the throat section and the inflow section respectively, D and D_{L0} are the diameter of pin fin and inflow section, $A_{\min}$ is the minimum passage area between two adjacent pin-fins, A_{L0} is the cross section area of inflow section, μ is the dynamics viscosity, and k is the thermal conductivity at the L_0 region.

Heat transfer coefficient prediction

Heat transfer coefficient (HTC) is calculated by equation 3 below.

$$h = \frac{q_{\mathrm{w}}}{\left(T_{\mathrm{w}} - T_{\mathrm{nw}}\right)} \tag{3}$$

Where h is the heat transfer coefficient, T_{w} is the wall temperature, T_{nw} is the near-wall fluid temperature, and q_{w} is the wall heat flux.

Pressure loss prediction

The pressure loss is evaluated from the 'cold' test simulation using adiabatic wall condition and ambient temperature of the inlet mainstream flow. The friction factor (f) as an expression of total pressure drop is formulated by the decrease of total pressure at the L_1 region over the averaged value of density and velocity in the L_0 region.

$$f = \frac{P_{\mathrm{L1-outflow}} - P_{\mathrm{L1-inflow}}}{0.5\rho v^2} \tag{4}$$

RESULTS AND DISCUSSION

Validation

The pressure 'cold' test simulation was performed using ANSYS-CFX to evaluate the friction factor within the coolant passage. It was carried out by steady RANS-SST turbulence modeling at an ambient temperature of 20^{o}C with varying inflow Reynolds number (Re_{L0}) between 9,000 and 36,000. Figure 2(a) gives simulation results of G5N21 and G5N22 configurations in comparison with experimental data. It shows that CFD predicted pressure losses are in good agreement with the experiment.

The 'warm' test is used to evaluate heat transfer coefficient (HTC) on the end-walls and the pin-fin surfaces. Simulation is performed at Re_{d5}=18,000 referring to Reynolds number at the throat section, the inflow temperature of 55.1^{o}C, and using the k-ε turbulence model. Figure 2(b) illustrates the lateral-averaged pin-fin HTC of streamwise and spanwise configurations, in comparison with the experimental data of Tarchi *et al*. [8]. It can be seen that the predicted pin-fin HTC of G5N21configuration agrees fairly well with the test data for all rows. However, for the G5N22 configuration, the predicted pin-fin HTC agrees well with the test data up to the 3rd row and it over-predicts HTC for remaining rows, resulting large discrepancies downstream for the last two rows. Despite this, CFD predicted pressure loss and pin-fin HTC are generally in good agreement with the test data, and the reasons that cause large deficits in predicting the G5N22 configuration need further investigations. Nevertheless, these validations will be served as a reference, in terms of mesh construction and model setting, for simulation further three geometries of shape change and orientation of pin-fin geometries, as described below.

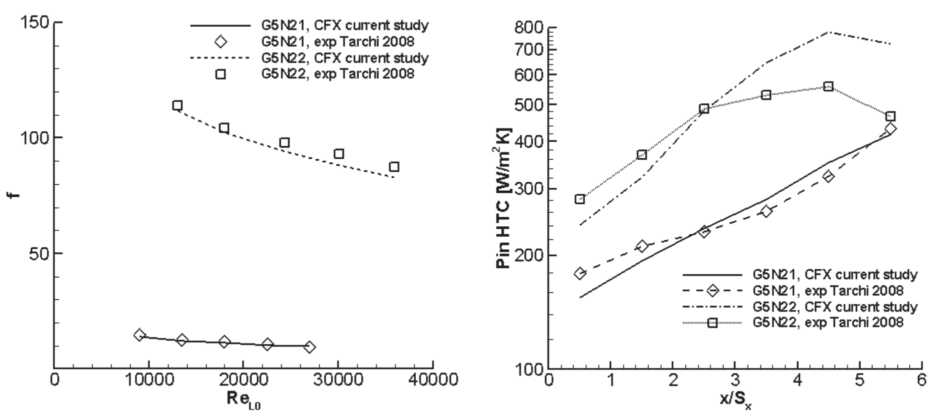

(a) Friction factor (b) Pin-fin HTC

FIGURE 2. Validation of total pressure loss and pin-fin HTC

Effect of pin-fin shape and orientation

Pressure loss and heat transfer coefficient

Figure 3(a) represents CFD predicted total pressure loss (friction factor) of five configurations. It can be clearly seen that for the G5N23 configuration with a rotating pin-fin angle of 45^o against incoming gas flow, the friction factor can be reduced up to max 67%, compared to that of the G5N22 configuration. The G5N24 configuration also achieves 60% reduction in the friction factor. Further decreases of 80% reduction in friction factor can be achieved by applying G5N10 and G5N21 configurations. However, these two configurations will produce lower HTC as discussed below.

Figure 3(b) gives the comparison of pin-fin HTC prediction for five configurations. By rotating the orientation of pin-fin angle of 45^o, i.e. G5N23 configuration, the pin-fin HTC can be increased up to 40%, compared to that of G5N21 configuration. G5N24 model also achieved similar level of higher pin-fin HTC. By considering the penalty of pressure loss, these two configurations can still be regarded as a compromise on achieving higher pin-fin HTC while keeping pressure loss to a minimum level.

Figure 3(c) shows the predicted end-walls HTC, using equation 3 above, for five configurations, respectively. It is evident that the G5N22 configuration produces the highest end-wall averaged HTC among all configurations, whereas the lowest end-wall averaged HTC is achieved by the G5N21 configuration, and the predicted HTC of G5N23 and G5N24 configurations are located in between, in consistent with that seen in Fig. 4b. These simulation results are consistent to a previous study of staggered short pin-fin arrays by van Fossen [16], who found that the pin-fin HTC is 35% higher than the end-wall HTC. Another research by Chyu [17] also noted that the pin-fin HTC is 10-20% higher than the end-wall HTC.

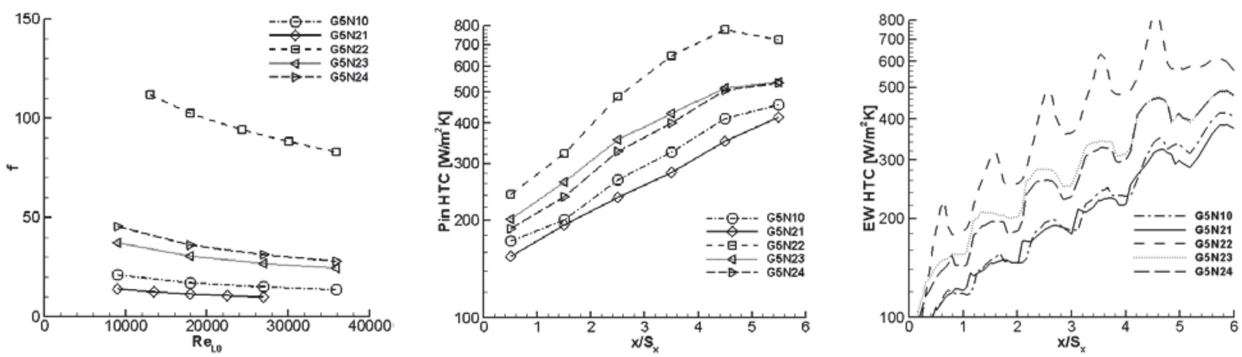

(a) Pressure loss (b) Pin-fin HTC (c) Pressure side wall HTC

FIGURE 3. Pressure loss and averaged HTC at varying pin-fin orientation

Nusselt number variations over L_0, L_1 and L_2 regions

Figure 4(a) indicates that in the L_0 region, Nusselt number (Nu) for all five configurations are almost the same, except the G5N23 configuration for which Nu is slightly higher than others four configurations. This indicates that there is insignificant effect of pin-fin orientation in the entrance L_0 region. In fact, the existence of pin-fin inside a coolant passage does affect the HTC, for example, simulation of an empty duct passage G5N00 shows a smaller HTC than those with passages equipped with pin-fins. The experiment of Facchini and Tarchi [18] also found that using enlarged pedestals and square or semicircular ribs will affect the Nusselt number.

Figure 4(b) gives Nu comparisons in the main L_1 region, where the existence of pin-fin is important in determining the heat transfer performance of the coolant passage. It is clear that the G5N22 model produces the highest Nu compared to others, whereas the G5N00 model of an empty duct produces the lowest Nu. This is consistent with experimental measurement as shown on the same graph. By rotating the pin-fin angle of 45^o against inflow either in-line (G5N23) or counter-rotating (G5N24), both configurations have shown a compromise performance in terms of pressure loss and heat transfer enhancement.

Figure 4(c) shows the results of comparison in the L_2 region. The magnitude of Nu continues to increase compared to that of the L_1 region. The 6^{th} row of fillet circular pin-fin in the L_2 region may contribute to heat transfer process due to increased surface area. However, to what extent it is caused by using a fillet circular pin-fin is not yet fully investigated in previous researches. It may need further simulations to quantify its influence.

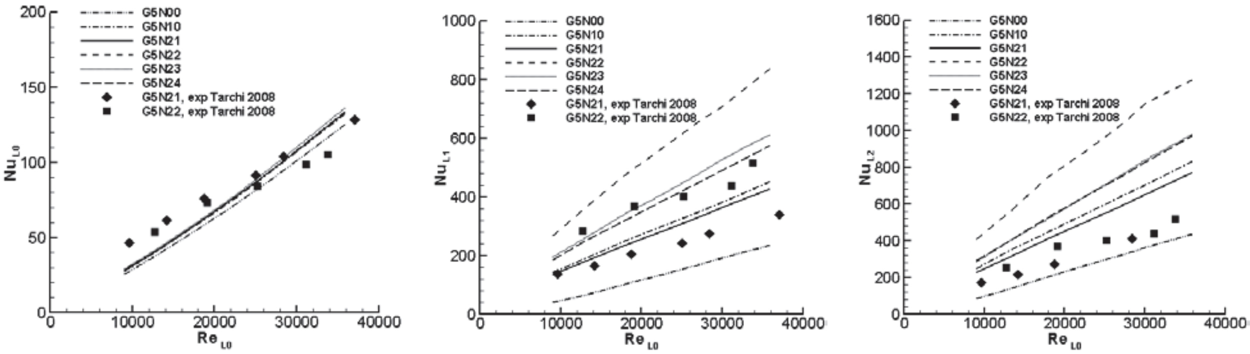

(a) L_0 (b) L_1 (c) L_2

FIGURE 4. Averaged Nusselt number over the L_0, L_1 and L_2 region

Turbulent levels and turbulent energy scale

Turbulent level (Tu) and turbulent energy scale (Lu) are evaluated by referring to 'warm test' simulation at Reynolds number 18,000. Initially, for all five configurations, the entrance flow has a low turbulence level of 0.62 – 1.12 % with a uniform velocity super-imposed at inlet. Turbulent level will increase gradually downstream after flow passing through each pin-fin row. Figure 5(a) shows the characteristics of turbulence level as a function of streamwise location of inlet and outlet and pin-fin rows. It is clear that the G5N22 model generates the highest turbulent level at the same streamwise position than that of other models, whereas the G5N21 model produces the lowest turbulent level. Fig. 5(b) gives the turbulent energy scale (Lu) and it seems that all configurations tend to remain near constant level throughout all five-row pin-fin in the L_1 region, with small variations between different configurations. This feature is similar to that observed by Ames *et al*. [19-20].

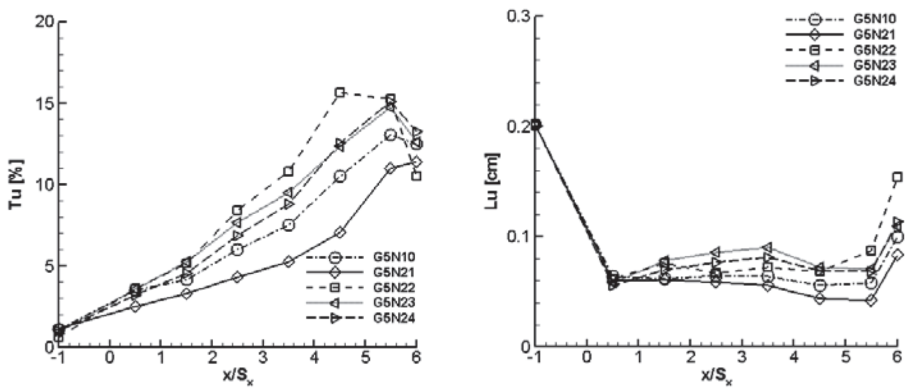

(a) Tu (b) Lu

FIGURE 5. Averaged turbulent levels and energy scale

Flow field visualization

The pin-fin cooling system works based on the principle of heat exchange like a heat exchanger. For any existence of temperature difference, an equilibrium condition will be achieved after the heat transfer process. Figure 6 shows trajectories of fluid particles from inlet plane travelling downstream towards exit plane. It is clear that uniformly distributed inflow in the L_0 is disturbed while approaching the pin-fin obstacles and the level of disturbance is dependent on the cross-section area of pin-fins. In the aft of pin-fin, flow separation occurs in the wake region and this will alter the local flow condition while approaching the next array of row, causing increased flow separation for downstream rows. It can be seen that for the spanwise pin-fin configuration (i.e., G5N22), the wake region is much wider than the streamwise pin-fin configuration (G5N21), with other three configurations have moderate wake region in size. The extent of flow separation will promote the turbulence intensity level that will further enhance the heat transfer performance.

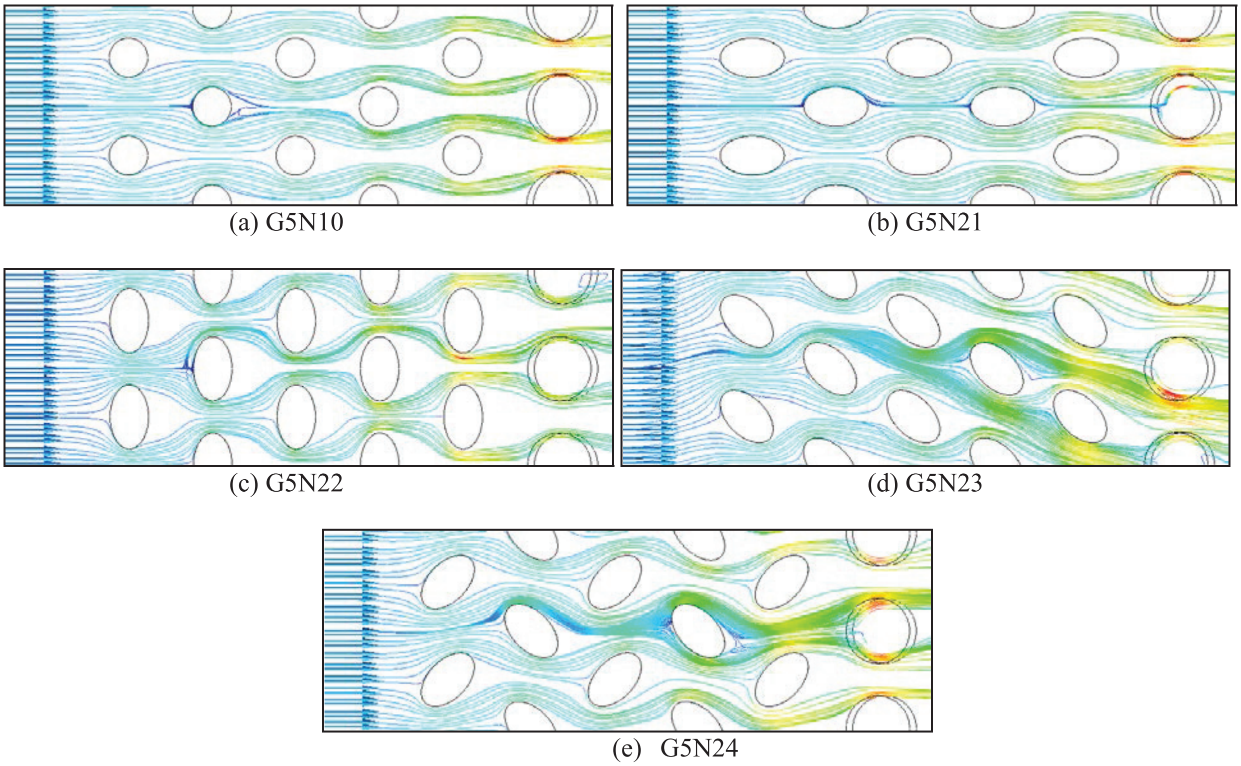

FIGURE 6. Trajectories of fluid particles from inlet travelling to exit in downstream

CONCLUSION

Heat transfer performance in turbine blade coolant passage has been studied numerically. Both CFD predicted heat transfer coefficient and pressure losses are in good agreement with the experimental data. The predicted friction factor representing the pressure losses has shown similar trend as the experimental data. In term of heat transfer coefficient prediction, the pin-fin HTC is always higher than that of the pressure side wall.

The elliptic pin-fin with against inflow produces compromised pressure loss and HTC between two baseline streamwise and spanwise elliptic pin-fin configurations. Therefore, this 45^{o} angle orientated configuration could be one of feasible solutions to enhance the HTC of pin-fin and end-walls, while keeping the pressure loss of the internal coolant passage to minimum level.

ACKNOWLEDGMENT

The first author would like to acknowledge the financial from Universitas Muhammadiyah Surakarta in supporting the collaboration research.

REFERENCES

[1] F. E. Ames, C. A. Nordquist and L. A. Klennert, "Endwall heat transfer measurement in a staggered pin fin array with an adiabatic pin," in *the ASME Turbo Expo 2007: Power For Land, Sea And Air, Montreal, Canada*, 2007.

[2] G. Delibra, D. Borello, K. Hanjalic and F. Rispoli, " URANS of flow and endwall heat tansfer in a pinned passage relevant to gas-turbine blade cooling," *J. Heat and Fluid Flow,* vol. 30, pp. 549-560, 2009.

[3] S. A. Lawson, A. A. Thrift, K. A. Thole and A. Kohli, "Heat transfer from multiple row arrays of low aspect ratio pin fin," *J. Heat and Mass Transfer,* vol. 54, pp. 4099-4109, 2011.

[4] O. Uzol and C. Camci, "Elliptical pin fins as an alternative to circular pin fins for gas turbine blade cooling applications-part 1: endwall heat transfer and total pressure loss characteristics," in *Proceedings of The ASME Turbo Expo International Gas Turbine Institute Conference*, New Orleans, La,USA, June 2001, ASME Paper No. GT-0180, 2001.

[5] O. Uzol and C. Camci, "Elliptical pin fins as an alternative to circular pin fins for gas turbine blade cooling applications-part 2: wake flow field measurements and visualization using particle image velocimetry," in *Proceedings of the ASME Turbo Expo International Gas Turbine Institute Conference*, New Orleans, La, USA, June 2001, ASME Paper No.GT-181, 2001.

[6] Y. Yao, M. Effendy, and J. Yao, "Evaluation of Wall Heat Transfer in Blade Trailing-edge Cooling Passage", *Applied Mechanics and Materials,* vol. 284-287, pp. 738-742, 2013

[7] M. Effendy, Y. Yao, and J. Yao, "Effect of Mesh Topologies on Wall Heat Transfer and Pressure Loss Prediction of a Blade Coolant Passage", *Applied Mechanics and Materials,* vol. 315, pp. 216-220, 2013.

[8] L. Tarchi, B. Facchini and S. Zecchi, " Experimental investigation of innovative internal trailing edge cooling configurations with pentagonal arrangement and elliptic pin fin," *J. Rotating Machinery,* no. Hindawi publisher, 2008.

[9] C. Bianchini, B. Facchini, F. Simonetti, L. Tarchi and S. Zecchi, " Numerical and experimental investigation of turning flow effects on innovative pin fin arrangements for trailing edge cooling configuration," *ASME Paper 2010-GT-23536*, 2010.

[10] M. Effendy, Y. Yao and J. Yao, "Comparison Study of Turbine Blade with Trailing-Edge Cutback Coolant Ejection Designs," in *51st AIAA Aerospace Sciences Meeting*, Grapevine, Texas, United States, 2013.

[11] M. Effendy, Y. Yao, J. Yao and D. R. Marchant, "Predicting Film Cooling Performance of Trailing–Edge Cutback Turbine Blades by Detached–Eddy Simulation," in *52nd AIAA Aerospace Sciences Meeting, SciTech 2014*, National Harbor, MD, United States, 2014.

[12] J. C. Han and A. Rallabandi, "Turbine blade film cooling using PSP technique," *Frontier In Heat and Mass Transfer (FHMT),* Vols. 1, 013001, pp. 1-21, 2010.

[13] N. F. Martin, J. J. Marra and S. S. Mellisa, "U.S. Patent 2011/0033311, A1". 2011.

[14] N. Sahiti, A. Lemouedda, D. Stojkovic, F. Durst and E. Franz, " Performance comparison of pin fin in-duct flow arrays with various pin cross-section," *J. Applied Thermal Engineering,* vol. 26, pp. 1176-1192, 2006.

[15] B. Facchini, F. Simonetti and L. Tarchi, " Experimental investigation of turning flow effects on innovative trailing edge cooling configurations with enlarged pedestals and square or semicircular ribs," *ASME Paper 2009-GT-59925*, 2009.

[16] G. J. Van Fossen, "Heat transfer coefficient for staggered arrays of short pin fins," *J. Engineering for Power,* vol. 104(2), pp. 268-274, 1982.

[17] M. K. Chyu, "Heat transfer and pressure drop for short pin fins arrays with pin-endwall fillet," *J. Heat Transfer,* vol. 112(4), pp. 926-932, 1990.

[18] B. Facchini and L. Tarchi, "Investigation of innovative trailing edge cooling configurations with enlarged pedestals and square or semicircular ribs - Part 1 experimental results.," *ASME Paper 2008-GT-51047*, 2008.

[19] F. E. Ames, L. A. Dvorak and M. J. Morro, "Turbulent augmentation of internal convection over pins in staggered-pin fin arrays," *J. Turbomachinery,* vol. 127, pp. 183-190, 2005.

[20] F. E. Ames and L. A. Dvorak, "Turbulent transport in pin fin arrays: experimental data and predictions," *J. Turbomachinery,* vol. 128, pp. 71-81, 2006.